JACC: ADVANCES VOL. 4, NO. 9, 2025

ORIGINAL RESEARCH

Machine Learning Reconstruction of Left Ventricular Pressure From Peripheral Waveforms

Alessio Tamborini, PhD,[a] Arian Aghilinejad, PhD,[a] Ray V. Matthews, MD,[b] Morteza Gharib, PhD[a]

ABSTRACT

BACKGROUND Left ventricular (LV) pressure measurement is the clinical gold standard for assessing cardiac function; however, its reliance on invasive catheterization limits accessibility and widespread use.

OBJECTIVES This study aimed to develop a cuff-based machine learning (cuff-ML) approach for reconstructing LV pressure from noninvasive brachial waveforms as a bedside assessment of cardiac function.

METHODS Subjects referred for nonemergent left heart catheterization were recruited for LV pressure and brachial cuff waveform measurement. The cuff-ML method was trained using brachial waveforms to predict LV pressure and was evaluated for morphology and parameters accuracy against invasive catheter measurements. Cardiac function was assessed based on the reduced LV peak pressure derivative ([+]dP/dt <1,200 mm Hg/s).

RESULTS A total of 104 subjects, comprising 3,572 simultaneous LV and cuff-based brachial waveform pairs, were analyzed using a 70:30 train-test split (test cohort: 32 subjects, 1,023 cardiac cycles). The cuff-ML approach demonstrated high accuracy in reconstructing LV waveform shape compared to catheter measurements (median normalized root mean squared error = 8.2%). Pressure-based parameters, including maximum pressure ($r = 0.92$, $P < 0.001$), mean blood pressure ($r = 0.94$, $P < 0.001$), and developed pressure ($r = 0.85$, $P < 0.001$), showed strong correlations with invasive measurements. Cuff-ML-reconstructed waveforms identified abnormal systolic contractility (72% sensitivity, 73% specificity) on a beat-to-beat basis.

CONCLUSIONS Cuff-ML accurately reconstructs LV pressure from brachial cuff measurements. This noninvasive approach may be helpful for assessment of cardiac function and requires further study. (JACC Adv. 2025;4:102104)

Assessing left ventricular (LV) pressure provides crucial insight into systolic and diastolic cardiac functions. Age-related and disease-induced myocardial impairment can lead to diminished LV contractile forces which culminate in cardiovascular disease and heart failure.[1,2] Clinicians rely on various parameters extracted from the LV waveform to diagnose and monitor such conditions. Systolic function evaluation assesses parameters such as the maximum pressure derivative ([+]dP/dt),

From the [a]Department of Medical Engineering, California Institute of Technology, Pasadena, California, USA; and the [b]Division of Cardiovascular Medicine, Keck School of Medicine, University of Southern California, Los Angeles, California, USA.
The authors attest they are in compliance with human studies committees and animal welfare regulations of the authors' institutions and Food and Drug Administration guidelines, including patient consent where appropriate. For more information, visit the Author Center.

Manuscript received May 12, 2025; revised manuscript received July 17, 2025, accepted July 18, 2025.

ISSN 2772-963X https://doi.org/10.1016/j.jacadv.2025.102104

ABBREVIATIONS AND ACRONYMS

BMI = body mass index

BP = blood pressure

COV = coefficient of variation

cuff-ML = cuff-based machine learning

ICC = intraclass correlation coefficient

LV = left ventricle/ventricular

MBP = mean BP

ML = machine learning

NN = neural network

nRMSE = normalized-root mean squared error

PWA = pulse waveform analysis

RMSE = root mean squared error

sSBP = suprasystolic blood pressure

SVR = support vector regression

which reflects ventricular contractility.[3] In addition, measuring LV end-systolic pressure provides insights into ventricular afterload, often combined with volumetric measurements to yield a load-independent measure of systolic performance.[4,5] For diastolic function, parameters like the maximum negative pressure derivative ([−] dP/dt) or the relaxation time constant (τ) are indicative of ventricular relaxation and can be affected in various cardiac pathologies.[6,7] Furthermore, LV end-diastolic pressure can be used to assess LV congestion.[8] A comprehensive analysis of the LV pressure waveform holds significant clinical utility.

Direct measurement of LV pressure requires left heart catheterization, an invasive procedure associated with some risk. Within cardiovascular pressure assessments, noninvasive peripheral measurements are routinely employed as surrogates for central pressures owing to their practical advantages in clinical settings.[9-13] Although primarily used for aortic parameters, peripheral waveforms can also potentially estimate a small subset of LV parameters.[14-16] However, the limited scope of these parameters significantly restricts their clinical applicability. There exists an unmet clinical need to develop a method that reconstructs the LV pressure waveform from noninvasive measurements at the peripheral arteries. Cuff-based systems represent an ideal platform for this application, harnessing their capabilities for repeatable and automated measurements, integrated pressure and waveform acquisition, and their extensive prevalence in clinical practice.[17,18]

To our knowledge, no well-established method currently exists for reconstructing the LV pressure waveform from noninvasive peripheral measurements. One of the primary challenges in this reconstruction is LV-aorta decoupling—the phase of the cardiac cycle during which the aortic valve is closed, preventing communication between the LV and the arterial system.[19-21] To address this gap, we developed a time-frequency machine learning (ML) approach designed to augment capturing the nonlinear dynamics of the decoupling phase. We evaluated our method using simultaneous data from invasive LV catheterization and noninvasive brachial cuff waveform measurements. The primary objective of this study is to develop a robust method for reconstructing the shape and magnitude of the LV pressure waveform using noninvasive peripheral measurements acquired with a simple brachial cuff. Our secondary aim is to assess accuracy and clinical relevance of parameters derived from the reconstructed LV waveform by comparing them against simultaneously acquired invasive reference measurements.

METHODS

STUDY DESIGN. This study involved concurrent pressure waveform measurements via invasive LV catheterization and noninvasive brachial cuff. Individuals aged 21 or older with a referral for nonemergent left heart catheterization were recruited between September 2021 and September 2022. The health centers that participated in the study included Princeton Baptist (Alabama), LSU Health Sciences Center (Louisiana), Long Beach Memorial Care Hospital System (California), Orange Coast Memorial Care Hospital (California), and Saddleback Memorial Care Hospital System (California). The study excluded participants who experienced a major adverse cardiac event within 1 week before catheterization, those in whom a brachial blood pressure (BP) measurement could not be obtained, and those in whom the interventional cardiologist contraindicated cardiac catheterization. Clinical data were collected via a chart review. The study received approval from 2 Institutional Review Boards (IRBs): the Western IRB and the Salus IRB. Before the procedure, participants provided written informed consent. The study adhered to the principles outlined in the Declaration of Helsinki.

STUDY DEVICES. Noninvasive pulse waveform recording was performed using an investigational brachial cuff device specialized for pulse waveform acquisition developed and validated by Tamborini and Gharib.[17,22] The cuff device consists of a noninvasive BP module for measurement functionalities and a custom pneumatic system for waveform capture. Device functionality—oscillometric BP measurement and tourniquet mode—were preprogrammed in the noninvasive BP module, all of which—methods and algorithms—were validated for accuracy and safety from the manufacturer. The cuff was designed to output results in analog format to a data acquisition system in real-time. The cuff protocol performs a BP measurement followed by pulse waveform capture using the tourniquet mode. The hold at suprasystolic BP (sSBP) was performed for 40 seconds, which is defined as systolic BP (SBP) plus 35 mm Hg. Calibration of the noninvasive waveforms followed previously described methods.[22] Briefly, each cuff-acquired waveform was first normalized and then linearly rescaled such that its maxima and minima correspond to the subject's SBP and diastolic BP, respectively, as obtained from the preceding oscillometric measurement using the same cuff device. The study required brachial cuff placement on the subject's left arm following standard cuff-placement guidelines.

Invasive pressure recording used the Millar Mikro-Cath pressure catheter. LV catheterization was performed via either femoral or radial access. Due to brachial cuff placement requirements, catheter access at the radial artery was restricted to the right site. A sampling frequency of 1 kHz was selected as it represents the highest rate supported by all study devices that falls within manufacturer operating recommendations to accurately capture rapid hemodynamic changes.

DATA HANDLING. Data were manually inspected and algorithmically filtered to exclude measurements affected by apparatus malfunction, procedural errors, saturated signals, arrhythmias, poor signal quality, or failure to identify waveform cardinal points. Subjects with missing data were dropped from the study. The data set comprised multiple pulse waveforms per subject, each treated as an individual but nonindependent data point. To prevent data leakage, we performed a *random subject-level train-test split*, assigning 70% of subjects to training and 30% to testing (**Figure 1C**). Model fitting and hyperparameter tuning were restricted to the training set, whereas the final evaluation was conducted on the held-out test set. To assess generalizability, we also conducted a 10-fold shuffle-split cross-validation using a fixed random seed, ensuring consistent 70:30 subject-level splits across folds (Supplemental Figure 1). Fourier decomposition reconstruction accuracy of the LV pressure was evaluated by transforming each waveform into the frequency domain and reconstructing it using a limited number of harmonics.

ALGORITHM DEVELOPMENT. Cuff-based ML (cuff-ML) was developed to map a calibrated brachial waveform during the sSBP hold to the corresponding LV pressure waveform. The input space included both time- ($n = 3$) and frequency-domain ($n = 35$) features. Time-domain features were derived using pulse wave analysis (PWA) to extract physiologically relevant characteristics. Frequency-domain features were obtained via Fourier transform, using the first 18 modes—defined by the sine and cosine coefficients of each harmonic component—of the brachial waveform. The model predicts the first 16 modes of the LV pressure waveform, which were converted back to the time domain using the inverse Fourier transform. Model training minimized the root mean squared error (RMSE) between predicted and reference LV waveforms in the time domain. The model architecture was a fully connected, feedforward neural network (NN) consisting of 3 dense layers (512, 256, and 64 nodes), trained for 60 epochs with a learning rate of 0.005. The model's 38 input features had no missing data. A detailed description is available in the Supplemental Notes.

The cuff-ML method was compared to a model developed using conventional Fourier-based ML transfer function principles, as previously outlined.[13,23] This ML approach relies exclusively on using frequency-domain information derived from Fourier decomposition to reconstruct the waveform at the target location. The model employs a support vector regression (SVR) architecture with 18 input modes, as originally proposed in the literature,[23] and 16 output modes to subsequently reconstruct the LV pressure waveform. The SVR model was configured with a linear kernel, a regularization parameter $C = 100$, and an ε-insensitive loss set at 0.001, all computed in the frequency domain. During the comparison, this model architecture will be referred to as SVR.

Both models were trained and tested on the same instances of training and testing cohorts. Methods were compared to evaluate waveform reconstruction accuracy on the testing population using the RMSE, normalized-RMSE (nRMSE), and Pearson Correlation Coefficient (r) metric. Real time applicability was evaluated by running the trained cuff-ML algorithm on an emulated stream of real data from individuals in the testing population. The algorithm iteratively searched for valid sSBP cuff waveforms in the data stream as input to cuff-ML for LV waveform prediction.

PWA was conducted on individual cardiac cycles for both the true and reconstructed LV waveforms. Subsequently, the results were subject averaged to generate a single prediction per individual. Clinically significant waveform parameters were extracted, inclusive of maximum pressure (P_{max}), mean BP (MBP), end systolic pressure, developed pressure, mean systolic pressure, (+)dP/dt, (−)dP/dt, contractility index, τ, tension-time index, isovolumic time, peak time (T_{peak}), systolic time (T_{sys}), and diastolic time (T_{dia}).[15,24-28] Supplemental Table 1 contains

FIGURE 1 **Cuff-ML Study Design**

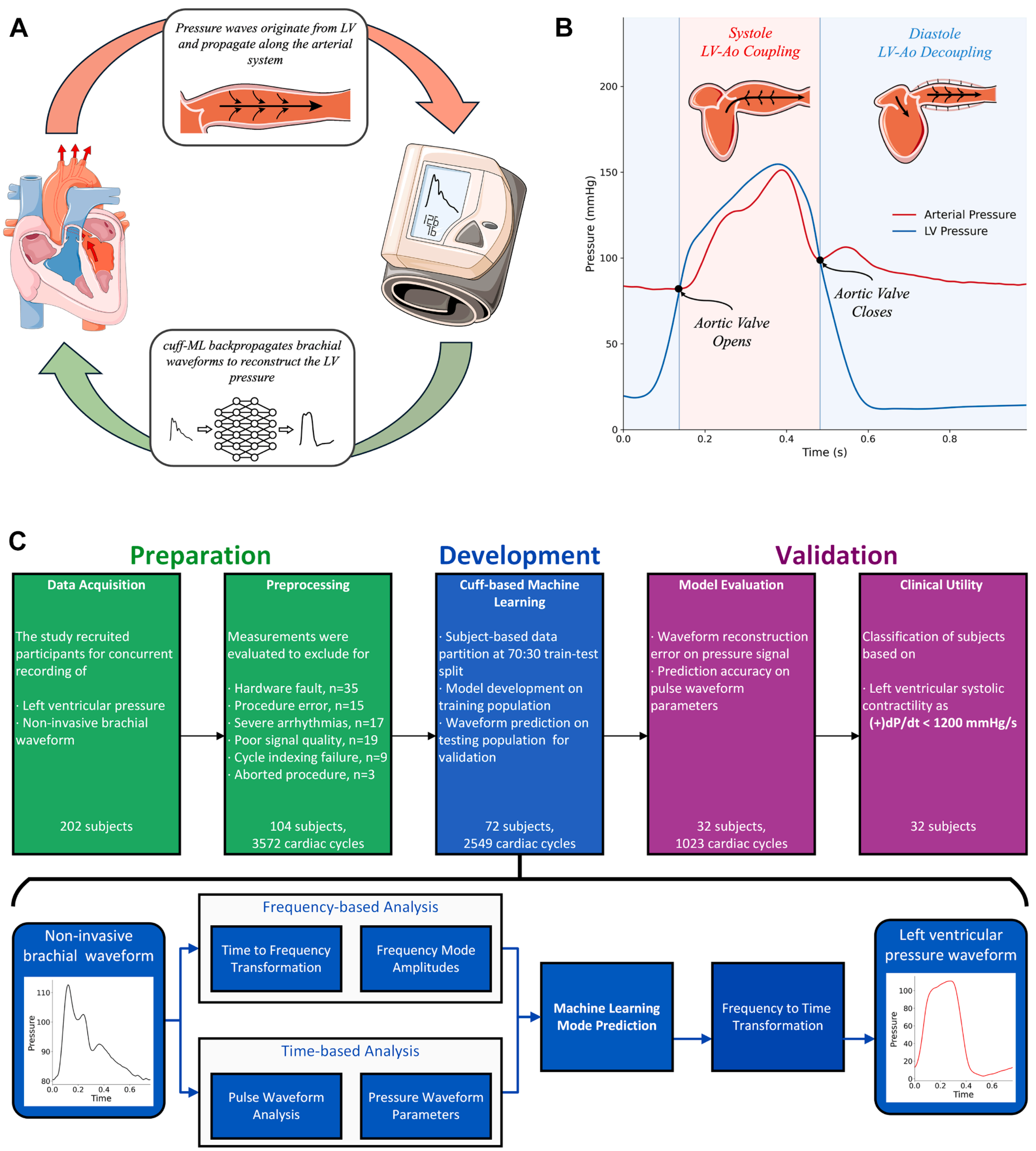

(A) Physiological wave propagation from LV to periphery and the reserve engineering approach of cuff-ML to reconstruct LV pressure. (B) Coupling and decoupling phases of the LV and arterial system via aortic valve opening and closing. (C) Study design and algorithm workflow for the cuff-ML models. Part of the figure was generated with adapted illustrations from Servier Medical Art, provided by Servier and licensed under a Creative Commons Attribution 3.0 Unported License. cuff-ML = cuff-based machine learning; LV-Ao = left ventricular-aorta.

parameter descriptions. Abnormal LV systolic contractility was assessed as (+)dP/dt at the threshold of 1,200 mm Hg/s.[29]

STATISTICAL ANALYSIS. Waveform reconstruction accuracy and shape correspondence were assessed using RMSE, nRMSE, and r between the true and reconstructed waveforms. The nRMSE expresses the error as a percentage, normalized by the pulse amplitude of the true signal. Cuff-ML was evaluated for reconstruction accuracy for individual cardiac cycles and the continuous signal. Individual cardiac cycle accuracy was assessed with RMSE and nRMSE on the pressure and first derivative. Evaluation of continuous pressure-time signal reconstruction assessed tracking accuracy in pressure fluctuations, reconstruction precision, and repeatability. Pressure tracking accuracy compared the average fluctuation of MBP during breathing cycles between the catheter and reconstructed signal. Cuff-ML waveform reconstruction consistency was assessed at the subject level by comparing the RMSE average and SD. Precision and repeatability were measured using the coefficient of variation, calculated as the ratio of the SD to the mean.

Parameters extracted using PWA on the reconstructed LV waveforms were assessed against true values obtained from catheter measurements using true-versus-predicted scatter plots and Bland-Altman analysis. Correlation strength was measured with r and with the intraclass correlation coefficient (ICC) reported with 95% CIs. Bland-Altman analysis was employed to determine bias and limits of agreement. Correlation between parameter residuals (true minus predicted) and covariates of age, body mass index (BMI), and body surface area was evaluated. The reconstructed LV pressure tracings were used to estimate abnormal systolic contractility, as measured with (+)dP/dt <1,200 mm Hg/s.[29] Classification analyses were performed on both the beat-to-beat level and the subject level. For subject-level classification, the final label was determined by averaging the classification across all cardiac cycles for a given patient, mimicking a clinical setting where multiple waveforms inform a single patient-level decision. Accuracy, sensitivity, and specificity were used to quantitatively assess the classification. Statistical differences were assessed using the nonparametric Mann-Whitney *U* test for continuous variables and the chi-square test for categorical variables. Statistical significance was set at $P < 0.05$. All analyses were conducted using custom scripts written in Python (version 3.11).

RESULTS

CLINICAL CHARACTERISTICS. Figure 1 summarizes the logic of the algorithmic approach, the problem statement, and the study design. The study initially recruited 202 individuals. After applying all exclusion criteria (ie, apparatus malfunction, procedural errors, saturated signals, arrhythmias, poor signal quality, or failure to identify waveform cardinal points), 104 subjects remained for analysis (Figure 1C), and none had missing data. The main exclusion included 18 cuff malfunctions, 17 severe arrhythmias, and 15 incorrect procedures (Figure 1C, Supplemental Table 2). The analysis cohort (n = 104) included 65% males, with an average age of 66 years and a mean BMI of 28.4 (Table 1). The study population reported high prevalence of hypertension (76%), hyperlipidemia (75%), and diabetes (33%). As part of the model development process, patients were divided into a training cohort (n = 72) and a testing cohort (n = 32). There were no statistically significant differences in patient characteristic between the 2 cohorts, as assessed using the Mann-Whitney *U* test and chi-square test (Supplemental Table 3). Supplemental Table 4 reports reasons for referral to catheterization. Processing the total study cohort (n = 104) generated 3,572 cardiac cycle pairs (cuff sSBP and LV catheterization). Supplemental Figures 2 and 3 evaluate the effect of limited modes on the self-reconstructed LV waveform, showing reconstruction accuracy using nRMSE (n = 3,572) and providing a visual representation, respectively. Supplemental Figure 4 reveals a 2-tailed distribution for the breathing-induced cardiac cycle start-to-end pressure difference with a mean of 0.0 (4.3) mm Hg. Supplemental Figure 5 highlights the morphological and magnitude variability of the LV pressure waveform within the study cohort.

CUFF-ML WAVEFORM RECONSTRUCTION. The cuff-ML model was independently fitted to the training population (subjects = 72; cardiac cycles = 2,549), and subsequently used to predict the LV waveform on the testing population (subjects = 32; cardiac cycles = 1,023). Reconstruction error was assessed in the test population (n = 1,023) using RMSE and nRMSE on the pressure signal in Figure 2A; the model yielded a median [IQR] RMSE of 9.9 [7.1, 14.1] mm Hg and nRMSE of 8.2 [5.8, 11.5] %. An example of a reconstructed and measured LV waveform is shown in Figure 2B with the respective error metrics. Figure 2C plots the one-to-one proportionality between measured and reconstructed waveforms on a

TABLE 1 Study Population

	All (N = 104)	Train (n = 72)	Test (n = 32)
Clinical characteristics			
Age (years)	66 ± 9	66 ± 9	64 ± 10
Male, n (%)	68 (65%)	44 (61%)	24 (75%)
Height, (m)	1.71 ± 0.10	1.71 ± 0.10	1.72 ± 0.09
Weight, (kg)	83.3 ± 17.5	82.7 ± 17.7	84.6 ± 17.3
Body mass index, (kg/m^2)	28.4 ± 5.1	28.2 ± 5.0	28.7 ± 5.2
White, n (%)	68 (65%)	46 (63%)	22 (68%)
Comorbidities			
Hypertension, n (%)	80 (76%)	53 (73%)	27 (84%)
Diabetes, n (%)	35 (33%)	24 (33%)	11 (34%)
Thyroid, n (%)	13 (12%)	12 (16%)	1 (3%)
Hyperlipidemia, n (%)	78 (75%)	54 (75%)	24 (75%)
Smoker, n (%)	14 (13%)	7 (9%)	7 (21%)
Cardiovascular disease			
Cardiomyopathy, n (%)	9 (8%)	5 (6%)	4 (12%)
Carotid artery disease, n (%)	26 (25%)	19 (26%)	7 (21%)
Heart valve disease, n (%)	18 (17%)	15 (20%)	3 (9%)
Aortic stenosis, n (%)	5 (4%)	4 (5%)	1 (3%)
Aortic regurgitation, n (%)	4 (3%)	4 (5%)	0 (0%)
Mitral stenosis, n (%)	0 (0%)	0 (0%)	0 (0%)
Mitral regurgitation, n (%)	13 (12%)	11 (15%)	2 (6%)
History of cardiac surgery, n (%)	12 (11%)	6 (8%)	6 (18%)
Myocardial infarction, n (%)	19 (18%)	15 (20%)	4 (12%)
Peripheral vascular disease, n (%)	20 (19%)	15 (20%)	5 (16%)
Pacemaker, n (%)	5 (4%)	4 (5%)	1 (3%)
Stroke, n (%)	2 (1%)	1 (1%)	1 (3%)

Values are mean ± SD unless otherwise indicated. Characteristics of the full study population with partition for the training (70%) and testing (30%) cohorts.

point-by-point basis for the test population. The cuff-ML model learning curve is reported Supplemental Figure 6.

The cuff-ML NN model is compared to a conventional Fourier-based ML model using the SVR architecture. Supplemental Figure 7 compares the reconstruction error of the 2 models on the pressure waveform and first derivative. For the pressure time signal, statistical analysis revealed significant difference between the SVR and NN models (RMSE: $P < 0.0001$; nRMSE: $P < 0.0001$; r: $P < 0.0001$). Similar trends were observed across the first derivative for RMSE, nRMSE, and r (Supplemental Figure 7). Supplemental Figure 8 showed the point-by-point proportionality plot for the 2 models.

Figure 3A displays the reconstructed waveform shape from cuff-ML in 4 individuals. The continuous LV pressure from cuff-ML closely follows the shape and pressure variations of the catheter measurement (**Figure 3B**). The cuff-ML reconstructed waveforms captured average MBP fluctuations from breathing (r = 0.77; $P < 0.0001$) as measured with the catheter (**Figure 3C**). The subject-level waveform reconstruction precision and repeatability generated a coefficient of variation of 0.28 (mean_{avg} = 10.8 mm Hg; SD_{avg} = 3.2 mm Hg). Supplemental Figure 9 shows continuous signal reconstructions for subject 2, subject 3, and subject 4 from **Figure 3A**. Supplemental Figure 10 displays 4 reconstructed and catheter waveforms with incremental RMSE. Supplemental Figure 11 displays the error distribution for MBP fluctuation amplitude and 3 cases of continuous signal reconstruction at incremental errors. Videos 1 to 4 show the real time implementation of cuff-ML for beat-to-beat prediction of LV pressure in 4 sample cases.

LV WAVEFORM ANALYSIS. PWA extracted clinically significant parameters from both the measured and reconstructed signals (n = 1,023). **Figures 4A and 4B** show the true-versus-predicted plots as well as the Bland-Altman analysis for 4 pressure-based parameters and 4 shape-based indices, respectively. All pressure-based parameters reported strong correlations between true and predicted values: P_{max} (r = 0.92; $P < 0.0001$; ICC: 0.96), MBP (r = 0.94; $P < 0.0001$; ICC: 0.96), end systolic pressure (r = 0.89; $P < 0.0001$; ICC: 0.94), and developed pressure (r = 0.85; $P < 0.0001$; ICC: 0.91). Shape-based indices also demonstrated strong correlations: T_{peak} (r = 0.85; $P < 0.0001$; ICC: 0.91), T_{sys} (r = 0.80; $P < 0.0001$; ICC: 0.89), tension-time index (r = 0.95; $P < 0.0001$; ICC: 0.97), and contractility index (r = 0.71; $P < 0.0001$; ICC: 0.79). Supplemental Figure 12 shows the analysis for 6 additional parameters measured on the LV pressure waveform using PWA. Supplemental Table 5 compares parameter residuals and covariates (age, BMI, and body surface area).

Reconstructed LV pressure waveforms were used to classify ventricular performance metrics on both a beat-to-beat and subject-averaged basis, using catheter measurements as reference (n = 1,023). Abnormal LV systolic contractility classification reported 563 true negative, 177 true positive, 218 false positive, and 65 false negative occurrences (**Figure 5A**), with an accuracy of 72% (sensitivity: 73%; specificity: 72%). The subject-averaged classification analysis yielded an accuracy of 75% (sensitivity: 89%; specificity: 70%) for abnormal LV systolic contractility (**Figure 5B**).

Model generalizability was tested with a 10-fold shuffle split validation on the entire study population (subjects = 104; cardiac cycles = 3,572); Supplemental Table 6 reports shuffle split data

FIGURE 2 Cuff-ML Reconstruction of LV Pressure

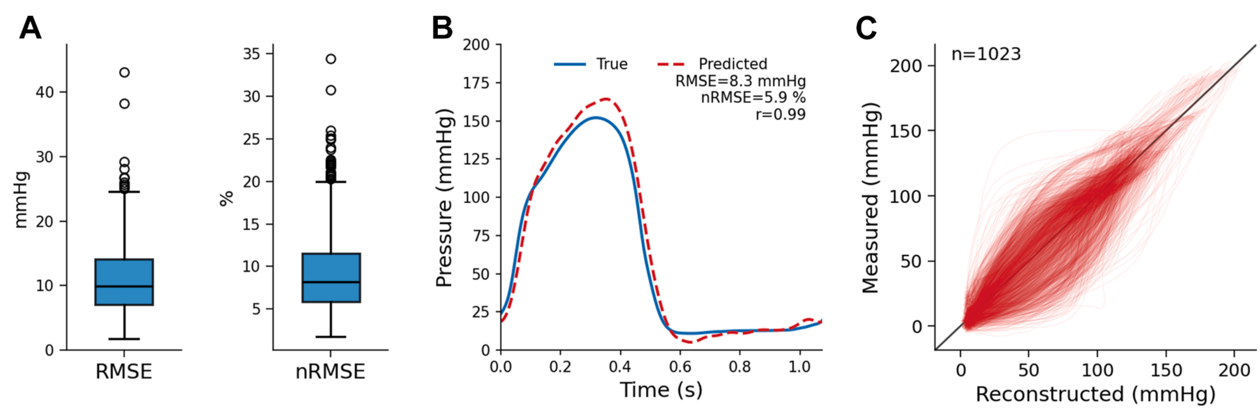

(A) Reconstruction error measured with the RMSE and the normalized nRMSE for the pressure signals. (B) A reconstructed waveform from the cuff-ML model against the measured waveform with annotated error metrics. (C) Shows the point-by-point proportionality plot between all measured and reconstructed waveforms. Black line represents the one-to-one proportionality. nRMSE = normalized-root mean squared error; RMSE = root mean squared error; other abbreviations as in Figure 1.

partitioning and Supplemental Table 7 reports waveform reconstruction error metrics of RMSE and nRMSE.

DISCUSSION

This study established that cuff-ML accurately and repeatably reconstructs LV pressure from noninvasive brachial waveform measurements. The cuff-ML method uses a nonlinear mapping technique to generate LV waveforms, with clearly defined systolic and diastolic segments. The results demonstrated that our reconstruction technique reliable captured patient-specific LV waveform magnitude and shape, our primary goal of this study. PWA on the cuff-ML reconstructed LV waveforms demonstrated strong correlations for pressure-based parameters and waveform indices when compared to catheter measurements. Analysis of the reconstructed waveforms classified cardiac cycles with abnormal systolic contractility using (+)dP/dt with a sensitivity of 72% and specificity of 73%. The **Central Illustration** summarizes the study objectives and results.

Previous studies aimed to reconstruct the LV waveform shape and magnitude but did not provide validated and applicable approaches in human subjects.[30,31] Xiao-Ping et al[30] developed a regression model in a population of ten dogs using only invasive measurements. Liu et al[31] developed a model on simulated, rather than measured, LV waveforms. To the best of the authors' knowledge, this study represents the first endeavor to reconstruct the LV waveform from noninvasive measurements in humans. We demonstrated that the LV waveform's morphology can be accurately captured using the Fourier transform. Using 16 modes, self-reconstruction achieved an nRMSE <1%, guiding our model's output dimensionality. We also confirmed that respiratory pressure fluctuations minimally affect cycle-to-cycle pressure deltas, validating the periodicity assumption and showing that Fourier decomposition introduces negligible bias. This work enhances the clinical use of peripheral measurements by introducing an ML technique to reconstruct the LV waveform—an approach that aligns with current trends in cardiovascular research.[32]

Noninvasive reconstruction of LV pressure is challenging due to the decoupling of the LV-aorta system following aortic valve closure during diastole. To address this limitation, we introduce 3 key technical enhancements to our previously proposed Fourier-based method which are aimed at augmenting model prediction in the diastolic segment.[13,23] Firstly, the cuff-ML model proposed in this paper uses a feed-forward NN architecture with fully connected layers, enabling it to capture complex nonlinear interactions among input parameters. In addition, the model incorporates time-domain features extracted from the pressure waveform using

FIGURE 3 **Continuous LV Waveform Reconstruction With Cuff-ML**

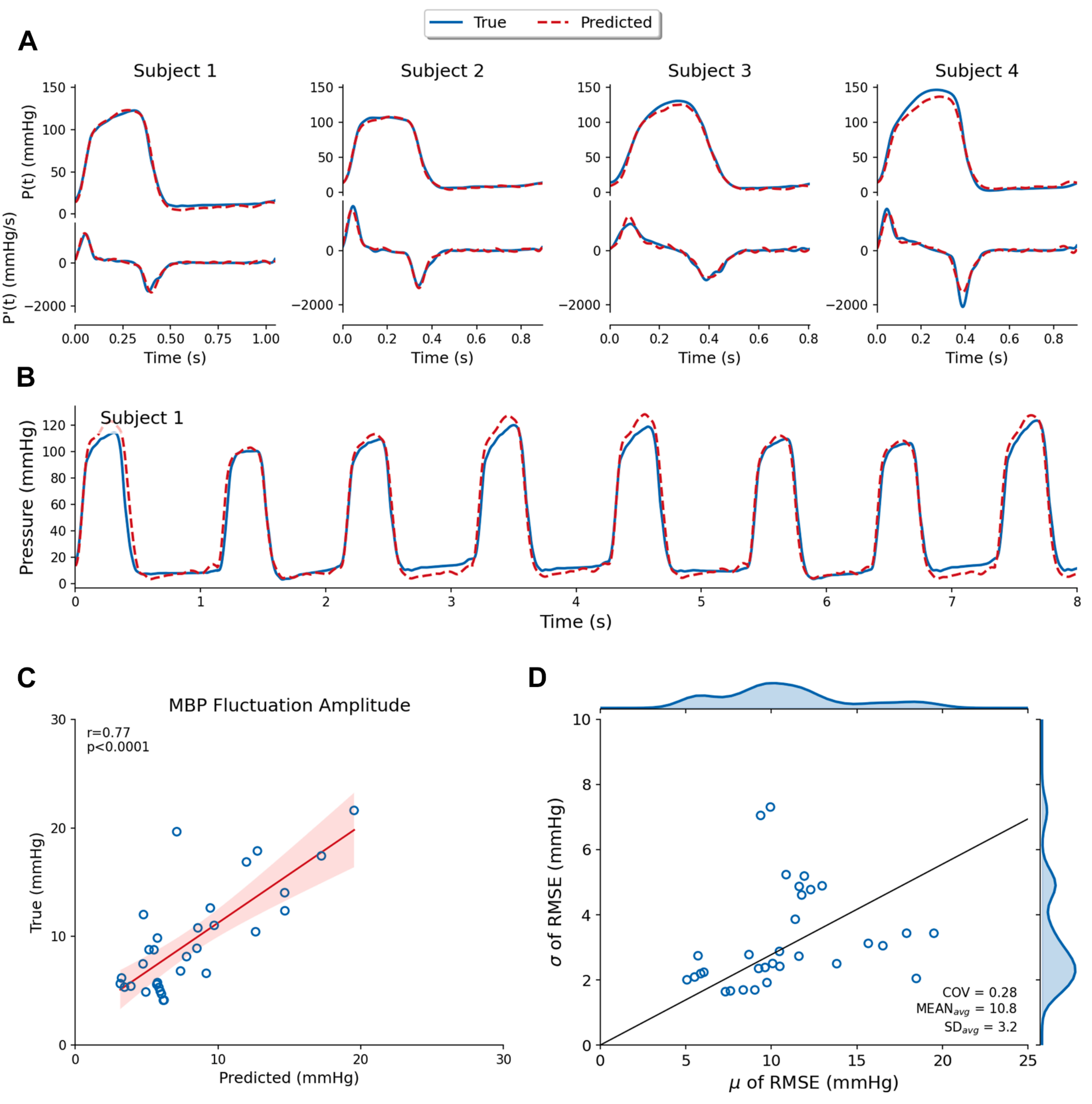

(A) LV pressure waveform and first derivative for catheter (true) and cuff-ML reconstruction (predicted) in 4 subjects. (B) A sample of the reconstructed continuous LV pressure signal using the cuff-ML method vs the catheter. (C) True-versus-predicted plot for the subject averaged LV mean pressure fluctuation amplitude across breathing cycles between the catheter measurement (true) and the cuff-ML reconstruction (predicted). (D) Quantifies the subject-level error and variability using the COV on the RMSE for the pressure signal reconstruction. COV = coefficient of variation; MBP = mean blood pressure; other abbreviations as in Figures 1 and 2.

PWA, specifically designed to capture waveform dynamics and enrich the input data space. Lastly, computing the loss function in the time domain directly on the reconstructed pressure-time signal ensures accurate representation of both systolic and diastolic components. To evaluate these improvements, we compared model performance of the proposed cuff-ML model with the SVR approach as described by Aghilinejad et al[23] and Tamborini et al.[33] This analysis demonstrated statistically significant

FIGURE 4 Comparison of True vs cuff-ML Measured LV Features

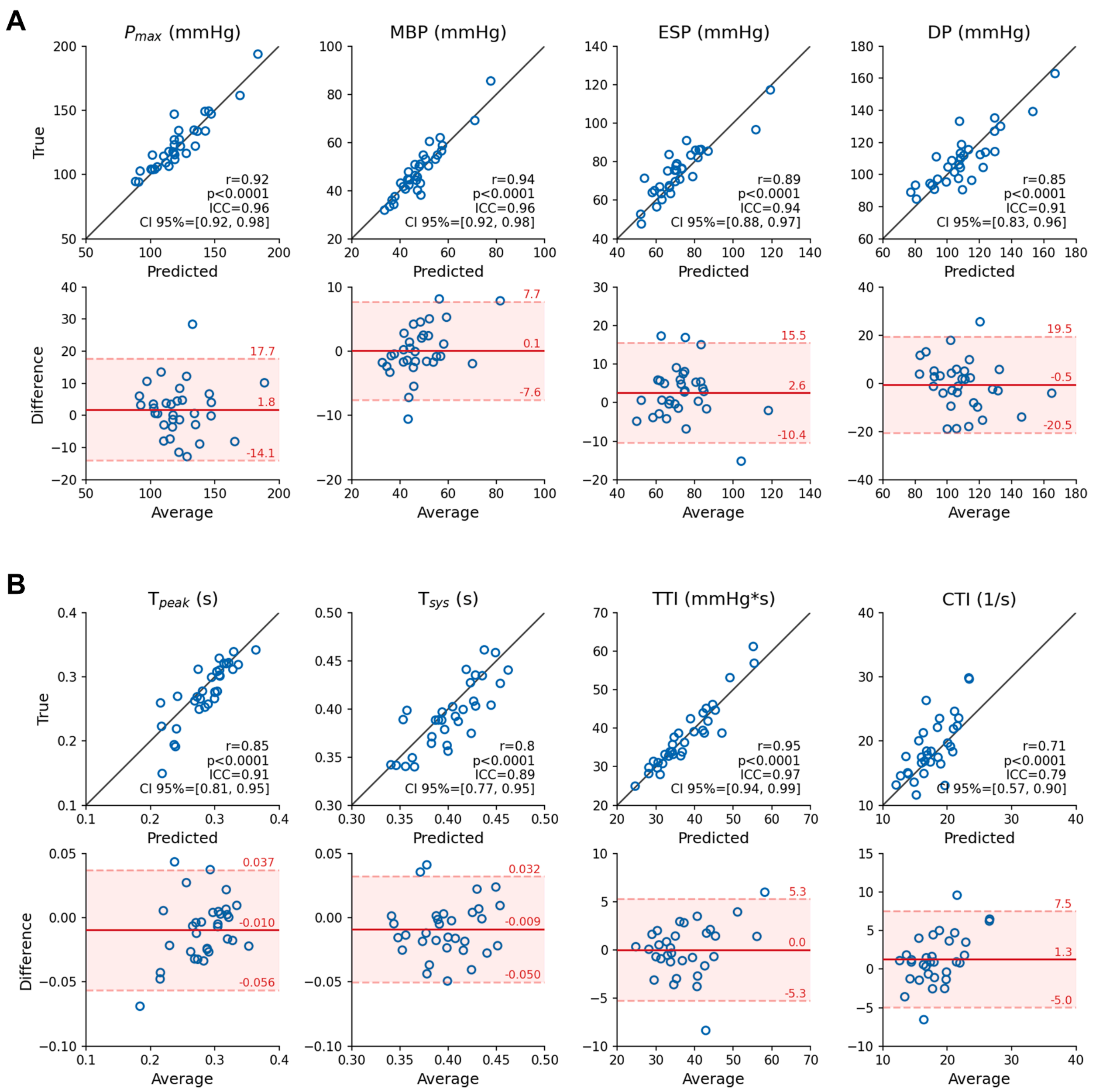

Prediction accuracy is evaluated using the true-versus-predicted and the Bland-Altman analysis of bias and 95% limits of agreement. (A) shows the pressure-based parameters, each column represents a different variable: maximum systolic pressure (P_{max}) in mm Hg; mean pressure (MBP) in mm Hg; end systolic pressure (ESP) in mm Hg; developed pressure (DP) in mm Hg. (B) shows the shape-based features, each column represents a different variable: peak timing (T_{peak}) in s; systolic time (T_{sys}) in s; time tension index (TTI) in mm Hg*s; contractility index (CTI) in 1/s. r = Pearson correlation coefficient; ICC = intraclass correlation coefficient; other abbreviations in Figure 1.

performance improvements across all reconstruction metrics on the pressure signal and its first derivative (Supplemental Figures 7 and 8). The technical advancements enhance explanatory power of the cuff-ML model effectively bridging the information gap between peripheral measurements and LV pressure.

LV waveforms reconstructed with cuff-ML display the expected pressure rise during contraction, fall

FIGURE 5 **Noninvasive Classification From the Reconstructed LV Pressure Waveform**

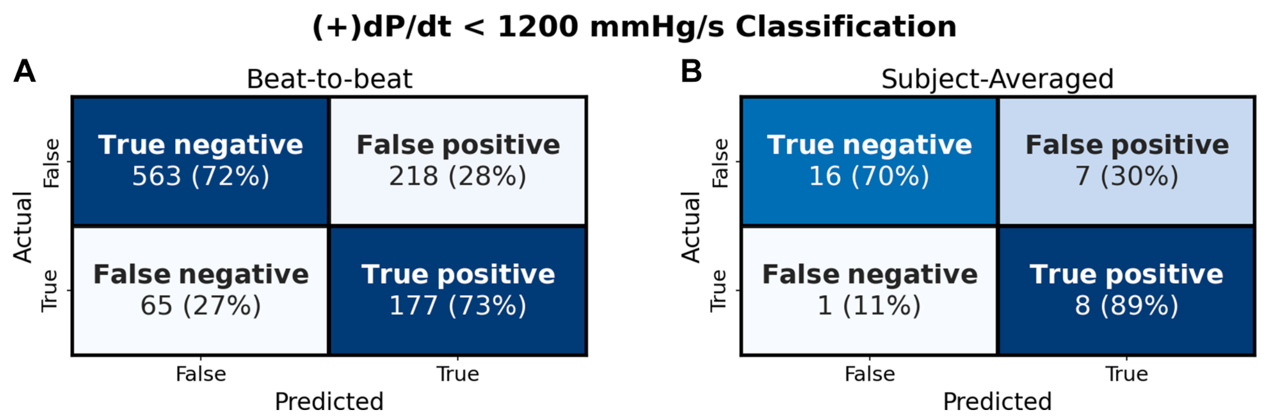

Shows the confusion matrix for LV contractility, defined at (+)dP/dt <1,200 mm Hg/s for the beat-to-beat (A) and subject averaged (B) analysis. Confusion matrix is normalized along the Actual rows.

during relaxation, and slow steady rise during filling (**Figure 3**). Similarly, the first derivative exhibits the isovolumetric contraction peak and isovolumetric relaxation dip as measured with a catheter. Supplemental Figure 10 further reveals that the waveform shape is well preserved across the full spectrum of prediction accuracies. The faithfulness of the reconstructed waveforms is also reflected in the continuous signal: the generated LV waveforms followed pressure and shape dynamics as measured invasively, indicating a high sensitivity to beat-to-beat pressure changes (**Figure 3**, Supplemental Figure 10). Most importantly, the deployment of cuff-ML on a data stream (Videos 1 to 4) demonstrated that the method could generate LV waveform predictions in real-time, allowing for clinical implementation at the patient's bedside. The cuff-ML reconstruction of LV pressure could have applications beyond pressure analysis, such as in the development of noninvasive pressure-volume loops. Previous methods found promising results using empirical, normalized, and noninvasively scaled reference curves for LV pressure; therefore, we anticipate that implementing a patient-specific LV pressure waveform from cuff-ML could significantly enhance such analyses.[34]

PWA was applied to the reconstructed LV waveforms to assess clinical applicability. The cuff-ML produced feature estimates that closely matched those measured with the catheter for most of the pressure, slope, area, and timing parameters. The strong predictions and low bias indicate that cuff-ML derived parameters are suitable for clinical analysis (**Figure 4**, Supplemental Table 5). It is noteworthy to discuss the marginally lower prediction accuracy observed for a subset of parameters, including τ and isovolumic time (Supplemental Figure 12). These parameters are measured on a portion of the pressure waveform during which the aortic valve is closed, aligning with the reduced information transmission from LV-aorta decoupling. Although this argument holds for some diastolic parameters, not all parameters in the diastolic segment were affected to the same extent. This variability may arise from the fact that only some of the LV properties are reflected in the peripheral waveform shape. Overall, the PWA results instill confidence in the predictive capabilities of cuff-ML, indicating their suitability for clinical decision-making.

The importance of measuring and monitoring different LV parameters as indicators of cardiac function is widely recognized.[3,16,35,36] For example, LV (+)dP/dt serves as a surrogate index of inotropic state and contractility.[8] Suzuki et al[25] reported lower (+)dP/dt is an independent predictor of cardiac mortality in patients with cardiac resynchronization therapy. It is further reported that in systolic heart failure, (+)dP/dt is reduced.[37] In this study, we evaluated the classification accuracy for the (+)dP/dt clinical threshold using the LV reconstructed

CENTRAL ILLUSTRATION Machine Learning Reconstruction of LV Pressure

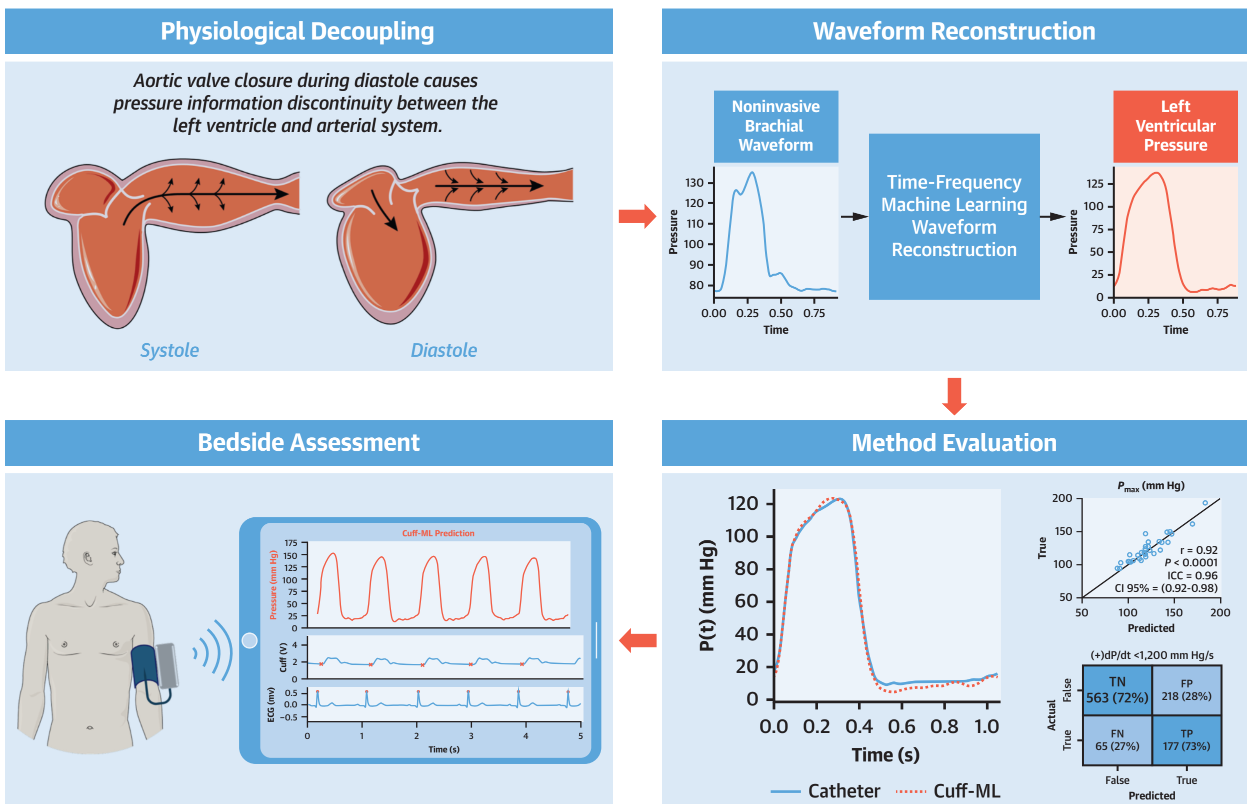

Tamborini A, et al. JACC Adv. 2025;4(9):102104.

cuff-ML = cuff-based machine learning; FN = false negative; FP = false positive; TN = true negative; TP = true positive.

waveform from cuff-ML. The cuff-ML reconstructed LV waveforms successfully classified cardiac cycles with abnormal systolic contractility with 72% accuracy. Using LV reconstructed waveforms from cuff-ML shows potential as a noninvasive tool for detecting abnormal cardiac function as measured with (+)dP/dt.

STUDY LIMITATIONS. Our study had some limitations. The cuff-ML model was developed and validated on a population referred for left heart catheterization, which is characterized by a high prevalence of cardiac conditions and comorbidities. For widespread clinical use, further validation is needed across diverse populations and conditions, including interventions that independently alter pressure (eg, inodilators, heart rate modulation, and volume loading) and patient populations with myocardial or vascular disease, abnormal ventricular-arterial coupling, or aging-related changes. Although this may limit the model's generalizability, the complex data set and analysis provides a strong foundation for such methods. Another limitation relates to data availability during algorithm development. Due to the high dimensionality of the data, we observed incremental performance improvements with increasing training size, suggesting that a larger data set could further enhance the model. Future studies with larger data sets can help refine the cuff-ML model and reveal its full potential.

CONCLUSIONS

We developed and validated a cuff-based method for reconstructing the LV pressure waveform from a noninvasive brachial measurement: cuff-ML. Our findings demonstrated accurate prediction of abnormal ventricular performance parameters as directly measured on the reconstructed waveform.

The trained cuff-ML method relies solely on a single point measurement at the brachial artery with a cuff-based system, which is widely accepted, automated, and noninvasive. This completely noninvasive technique holds the promise of providing inexpensive, real-time information on ventricular performance and requires further study.

FUNDING SUPPORT AND AUTHOR DISCLOSURES

Dr Tamborini is a consultant for Avicena LLC but declares no nonfinancial competing interests. Dr Gharib is a co-founder of Avicena LLC but declares no nonfinancial competing interests. All other authors have reported that they have no relationships relevant to the contents of this paper to disclose.

ADDRESS FOR CORRESPONDENCE: Dr Alessio Tamborini, Department of Medical Engineering, California Institute of Technology, 1200 E California BLVD, Pasadena, California 91125, USA. E-mail: atambori@caltech.edu.

PERSPECTIVES

COMPETENCY IN SYSTEM-BASED PRACTICE: Cuff-ML enables noninvasive, beat-to-beat reconstruction of LV pressure waveforms from brachial cuff waveform measurements, offering clinicians an accessible and automated tool for a preliminary assessment of cardiac function without the need for invasive catheterization.

TRANSLATIONAL OUTLOOK: Future studies will need to assess the generalizability and clinical applicability of this ML method for detecting cardiac function parameters across broader patient populations. Demonstrating its effectiveness in diverse care settings will be critical for widespread clinical adoption and integration into routine cardiovascular assessment.

REFERENCES

1. Li H, Hastings MH, Rhee J, Trager LE, Roh JD, Rosenzweig A. Targeting age-related pathways in heart failure. *Circ Res*. 2020;126:533–551.

2. Senni M, Redfield MM. Congestive heart failure in elderly patients. *Mayo Clinic Proceedings*. 1997;72:453–460.

3. Mason DT. Usefulness and limitations of the rate of rise of intraventricular pressure (dp/dt) in the evaluation of myocardial contractility in man. *Am J Cardiol*. 1969;23:516–527.

4. Hausdorf G, Gluth J, Nienaber CA. Non-invasive assessment of end-systolic pressure-length and stress-shortening relationships in normal individuals: significance of different loading conditions induced by methoxamine and angiotensin II. *Eur Heart J*. 1987;8:1099–1108.

5. Chen C-H, Fetics B, Nevo E, et al. Noninvasive single-beat determination of left ventricular end-systolic elastance in humans. *J Am Coll Cardiol*. 2001;38:2028–2034.

6. Eichhorn P, Grimm J, Koch R, Hess O, Carroll J, Krayenbuehl HP. Left ventricular relaxation in patients with left ventricular hypertrophy secondary to aortic valve disease. *Circulation*. 1982;65:1395–1404.

7. Thompson DS, Wilmshurst P, Juul SM, et al. Pressure-derived indices of left ventricular isovolumic relaxation in patients with hypertrophic cardiomyopathy. *Heart*. 1983;49:259–267.

8. Poyanmehr R, Hanke JS, Boethig D, et al. Validity and accuracy of the derived left ventricular end-diastolic pressure in impella 5.5. *Circ Heart Fail*. 2025:e012154.

9. Terentes-Printzios D, Gardikioti V, Vlachopoulos C. Central over peripheral blood pressure: an emerging issue in hypertension research. *Heart Lung Circ*. 2021;30:1667–1674.

10. Aghilinejad A, Tamborini A, Gharib M. Abstract 4142004: predicting cardiovascular disease events using uncalibrated non-invasive carotid pressure wave components from spectral regression learning. *Circulation*. 2024;150:A4142004.

11. Aghilinejad A, Gharib M. Assessing pressure wave components for aortic stiffness monitoring through spectral regression learning. *Eur Heart J Open*. 2024;4:oeae040.

12. Catino AB, Hubbard RA, Chirinos JA, et al. Longitudinal assessment of vascular function with sunitinib in patients with metastatic renal cell carcinoma. *Circ Heart Fail*. 2018;11:e004408.

13. Tamborini A, Aghilinejad A, Gharib M. A spectral machine learning approach to derive central aortic pressure waveforms from a brachial cuff. *Proc Natl Acad Sci U S A*. 2025;122:e2416006122.

14. Pauca AL, O'Rourke MF, Kon ND. Prospective evaluation of a method for estimating ascending aortic pressure from the radial artery pressure waveform. *Hypertension*. 2001;38:932–937.

15. Kappus RM, Ranadive SM, Yan H, et al. Validity of predicting left ventricular end systolic pressure changes following an acute bout of exercise. *J Sci Med Sport*. 2013;16:71–75.

16. Ostadal P, Vondrakova D, Krüger A, Janotka M, Naar J. Continual measurement of arterial dP/dtmax enables minimally invasive monitoring of left ventricular contractility in patients with acute heart failure. *Critical Care*. 2019;23:364.

17. Tamborini A, Gharib M. A pneumatic low-pass filter for high-fidelity cuff-based pulse waveform acquisition. *Ann Biomed Eng*. 2023;51:2617–2628.

18. Muntner P, Shimbo D, Carey RM, et al. Measurement of blood pressure in humans: a scientific statement from the American Heart Association. *Hypertension*. 2019;73:e35–e66.

19. Cooper LL, Rong J, Pahlevan NM, et al. Intrinsic frequencies of carotid pressure waveforms predict heart failure events: the Framingham heart study. *Hypertension*. 2021;77:338–346.

20. Manisty C, Mayet J, Tapp RJ, et al. Wave reflection predicts cardiovascular events in hypertensive individuals independent of blood pressure and other cardiovascular risk factors: an ASCOT (Anglo-Scandinavian cardiac outcome trial) substudy. *J Am Coll Cardiol*. 2010;56:24–30.

21. Safar M, O'Rourke MF. *Arterial stiffness in hypertension*. Edinburgh: Elsevier; 2006.

22. Tamborini A, Gharib M. Validation of a suprasystolic cuff system for static and dynamic representation of the central pressure waveform. *J Am Heart Assoc*. 2024;13:e033290.

23. Aghilinejad A, Tamborini A, Gharib M. A new methodology for determining the central pressure waveform from peripheral measurement using Fourier-based machine learning. *Artif Intell Med*. 2024:102918.

24. Yamamoto K, Masuyama T, Tanouchi J, et al. Importance of left ventricular minimal pressure as a determinant of transmitral flow velocity pattern in the presence of left ventricular systolic dysfunction. *J Am Coll Cardiol*. 1993;21:662–672.

25. Suzuki H, Shimano M, Yoshida Y, et al. Maximum derivative of left ventricular pressure predicts cardiac mortality after cardiac resynchronization therapy. *Clin Cardiol*. 2010;33:E18–E23.

26. Weisfeldt M, Scully H, Frederiksen J, et al. Hemodynamic determinants of maximum negative dP-dt and periods of diastole. *Am J Physiol*. 1974;227:613–621.

27. Adler D, Scott Monrad E, Sonnenblick EH, Hess OM, Krayenbuehl HP. Time to dp/dtmax, a useful index for evaluation of contractility in the catheterization laboratory. *Clin Cardiol*. 1996;19:397-403.

28. Weiss JL, Frederiksen JW, Weisfeldt ML. Hemodynamic determinants of the time-course of fall in canine left ventricular pressure. *J Clin Invest*. 1976;58:751-760.

29. Chengode S. Left ventricular global systolic function assessment by echocardiography. *Ann Card Anaesth*. 2016;19:S26-S34.

30. Hu XP, Chen JQ, Zhou ZN, Hu ST. Estimation of entire cardiac left ventricular pressure cycle from brachial arterial pressure during systemic hypoxia. *Proc Annu Symp Comput Appl Med Care*. 1991:446-449.

31. Liu J, Hao L, van de Vosse F, Xu L. A noninvasive method of estimating patient-specific left ventricular pressure waveform. *Comput Methods Programs Biomed*. 2022;227:107192.

32. Quer G, Arnaout R, Henne M, Arnaout R. Machine learning and the future of cardiovascular care. *JACC*. 2021;77:300-313.

33. Tamborini A, Aghilinejad A, Gharib M. Abstract 4141635: reconstructing invasive aortic pressure waveforms from non-invasive brachial measurements using a machine learning approach. *Circulation*. 2024;150:A4141635.

34. Russell K, Eriksen M, Aaberge L, et al. A novel clinical method for quantification of regional left ventricular pressure-strain loop area: a non-invasive index of myocardial work. *Eur Heart J*. 2012;33:724-733.

35. Kass DA, Maughan WL, Guo ZM, Kono A, Sunagawa K, Sagawa K. Comparative influence of load versus inotropic states on indexes of ventricular contractility: experimental and theoretical analysis based on pressure-volume relationships. *Circulation*. 1987;76:1422-1436.

36. Kolias TJ, Aaronson KD, Armstrong WF. Doppler-derived dP/dt and −dP/dt predict survival in congestive heart failure. *J Am Coll Cardiol*. 2000;36:1594-1599.

37. Aurigemma GP, Zile MR, Gaasch WH. Contractile behavior of the left ventricle in diastolic heart failure. *Circulation*. 2006;113:296-304.

KEY WORDS brachial cuff, catheterization, left ventricular pressure, machine learning, peripheral waveforms, transfer function

APPENDIX For supplemental notes, tables, figures, and videos, please see the online version of this paper.